Available online at www.sciencedirect.com
ScienceDirect
Thermochimica Acta 461 (2007) 67–71
thermochimica acta
www.elsevier.com/locate/tca

# Aging effects on the thermal expansion coefficient and the heat capacity of glassy polystyrene studied with simultaneous measurement using temperature modulation technique

Koji Takegawa, Koji Fukao, Yasuo Saruyama *

*Division of Macromolecular Science and Engineering, Kyoto Institute of Technology, Matsugasaki, Sakyo 606-8585 Kyoto, Japan*

Available online 27 April 2007

**Abstract**

Aging effects on the glassy polystyrene were studied with simultaneous measurement of the complex thermal expansion coefficient and the complex heat capacity. Aging period was changed from 10 to 100 h at 90 °C. It was found that the stepwise change in the real part of the complex thermal expansion coefficient and the peak of the imaginary part occurred at lower temperature than those of the complex heat capacity in all cases. As the aging period increased the stepwise change in the real part shifted to the higher temperature and sharpened. A qualitative model based on the energy landscape picture is proposed.


*Keywords:* Thermal expansion coefficient; Heat capacity; Simultaneous measurement; Temperature modulation technique

## 1. Introduction

Aging of glassy materials just below the glass transition temperature has been studied extensively [1]. Aging effects appear as change in temperature dependence of material properties such as volume, thermal expansion coefficient, heat capacity, dielectric coefficient and so on. Temperature dependence of these properties changes with the aging condition such as temperature and time. Comparison of the aging effects on different properties will provide useful information to understand the aging phenomena and the slow dynamics characterizing the glass transition. However, reliable comparison is often difficult because the material properties are sensitive to the thermal history. If two kinds of properties are measured independently non-negligible difference in the aging condition and/or the heating/cooling rate before and after the aging are difficult to be avoided. Such difference in the experimental condition makes the comparison less reliable.

In order to solve this problem an instrument for simultaneous measurement of the thermal expansion coefficient and the heat capacity has been developed in the authors' laboratory [2]. Since this instrument uses the temperature modulation technique it will be called temperature modulated expansion and heat capacity (Ex-HC) meter below. A simultaneous measurement of the thermal expansion coefficient, the heat capacity and the compressibility has been carried out by Takahara et al. [3]. They used an adiabatic type instrument. The adiabatic technique and the temperature modulation technique are complementary to each other. Our study is aimed to investigate the aging effects. As mentioned above the heating and cooling processes as well as the isothermal aging can affects the sample properties. In order to minimize the effects from the heating and cooling processes the heating and cooling rate should be high. The temperature modulation technique is more suitable to achieve the high heating/cooling rate than the adiabatic technique because the sample dimension of our instrument is much smaller than that of the adiabatic instrument.

The temperature modulated Ex-HC meter provides the complex thermal expansion coefficient and the complex heat capacity. The complex heat capacity has been measured with the temperature modulated differential scanning calorimeter (TMDSC) in the studies of the melting [4], the crystallization [5] and the glass transition [6,7] of polymers. The complex thermal expansion coefficient $\alpha^*$ is defined similarly to the complex heat capacity as given by the next equation.

$$\alpha* = \frac{1}{V}\frac{A_V}{A_T} \tag{1}$$

* Corresponding author. Tel.: +81 75 724 7738; fax: +81 75 724 7738.
*E-mail address:* saruyama@kit.ac.jp (Y. Saruyama).

0040-6031/$ – see front matter © 2007 Elsevier B.V. All rights reserved.
doi:10.1016/j.tca.2007.04.017

where $V$ is the volume of the sample. $A_V$ and $A_T$ are the complex amplitude of the sinusoidal modulation of the volume and the temperature, respectively. In this work the thickness of the sample was measured with the capacitive dilatometry which is a technique to evaluate the sample thickness from the electric capacitance [8,9]. Thermal expansion coefficient has been measured with temperature modulation by Price using TMA [10–12] and by Kamasa et al. using an instrument for a rod shaped sample [13–16]. Since the capacitive dilatometry can measure the thickness change of a thin sample it fits the temperature modulation technique particularly at high frequencies.

## 2. Experimental

The sample was atactic polystyrene (at-PS) of $Mw = 2.8 \times 10^5$. Pellets of at-PS were heated in air on a hot plate and pressed just after passing the glass transition temperature to form a disk of 1.5 mm thickness in less than 10 s. The disk was further pressed at 230 °C between two glass plates for 12 h in a vacuum chamber. The final film of 66 μm thickness was used as the sample.

The design of the detector was modified from the previous one [2] as shown in Fig. 1. A glass plate of 0.15 mm thickness was used as the base plate. A and B are the samples cut from the same sheet. C and D are aluminum films of 150 nm thickness made with vacuum deposition on the top surface of the base plate. C and D are the detector for the calorimetry and the lower electrode for the electric capacitance measurement, respectively. A and B were put on C and D, respectively, and the detector was kept at

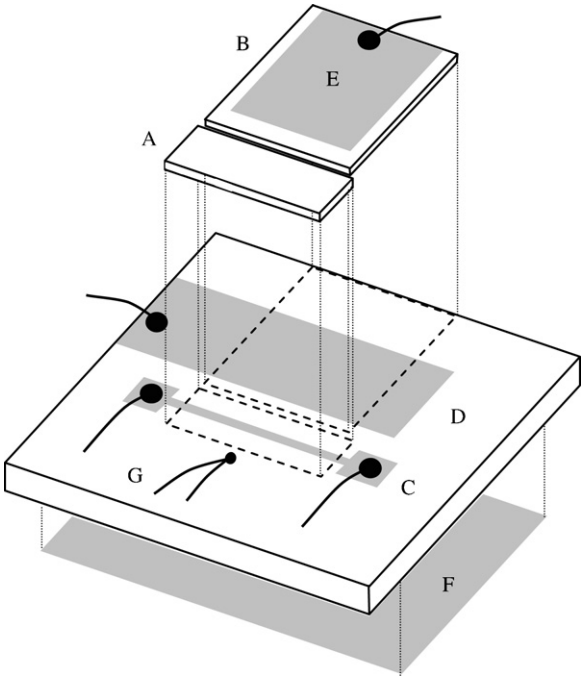


Fig. 1. A diagram of the sample and the detector. (A, B) samples for the calorimetry and the capacitive diratometry, respectively, (C) thermometer for the temperature modulation, (D, E) the lower and the upper electrode for capacitance measurement, respectively, (F) heater for the temperature modulation, (G) thermocouple.

150 °C for 8 h in the vacuum chamber to make the samples be in good contact with the aluminum films. Then aluminum film E of 150 nm thickness was made by vacuum deposition on the top surface of B as the upper electrode for the electric capacitance measurement. The effective area of the capacitor was 450 $mm^2$. On the bottom surface of the base plate, aluminum film F of 150 nm thickness was vacuum deposited as the heater for the temperature modulation. Black circles show the points where electric lead wires were connected. The thermocouple G was used to measure the temperature averaged over one modulation period. The detector was placed in a cell whose temperature was controlled linearly with time. The temperature on the sample surface of the previous detector was not sufficiently uniform for detailed comparison of the thermal expansion coefficient and the heat capacity. In the present instrument the temperature distribution was within ±0.2 K which was achieved with making the area of the samples smaller and optimizing the geometric arrangement on the base plate.

The electric capacitance was measured with an impedance analyzer (HP4294). Frequency of the electric field was 100 kHz, which was sufficiently high to avoid non-negligible effects from dispersion phenomena. The method to calculate the sample thickness from the electric capacitance was described in reference [1]. The thermal expansion coefficient attributed to the linear heating, which will be called total thermal expansion coefficient below, was calculated from the volume averaged over one modulation period and the temperature measured with the thermocouple G. The complex thermal expansion coefficient was calculated from the complex amplitude of the periodic change of the thickness and the complex amplitude of the temperature modulation measured with the detector C.

The complex heat capacity was calculated as follows. Assuming that the heat drain from the sample surface to the air is proportional to the sample temperature the next mathematical model was obtained.

$$C^* \frac{dT_{ac}}{dt} = K_h P - K_d T_{ac} \tag{2}$$

where $C^*$, $T_{ac}$, $t$ and $P$ are the complex heat capacity of the sample, the periodic component of the temperature, time and the periodic component of the power of the heater F in Fig. 1, respectively. $K_h$ and $K_d$ are coefficients of correction for the heater power and the heat drain. $P$ was calculated from the voltage of the power supplier and the electric current passing the heater. Correction with $K_h$ was necessary because the power supplied to the sample was not exactly equal to $P$ because of the heat diffusion through the base plate. It was assumed that $C^* = C^*_{liq} + C_{gl}$ where $C^*_{liq}$ was the liquid component or the configurational component and $C_{gl}$ was the glass component. Eq. (2) became

$$C^*_{liq} = |K_h| \left( \frac{\exp(i\theta_h) P}{i\omega T_{ac}} - \frac{i\omega C_{gl} + K_d}{i\omega |K_h|} \right) \tag{3}$$

where $\theta_h$ is the phase of $K_h$. It was further assumed that the second term in the parentheses could be expressed by a linear

function of the average temperature $T$ in good approximation.

$$C^*_{\mathrm{liq}} = |K_{\mathrm{h}}| \left( \frac{\exp(\mathrm{i}\theta_{\mathrm{h}})P}{\mathrm{i}\omega T_{\mathrm{ac}}} - (\xi_1 T + \xi_0) - \mathrm{i}(\eta_1 T + \eta_0) \right) \quad (4)$$

where $\eta_0$, $\eta_1$, $\xi_0$ and $\xi_1$ are real valued constants. Values of $|K_{\mathrm{h}}|$, $\theta_{\mathrm{h}}$, $\eta_0$, $\eta_1$, $\xi_0$ and $\xi_1$ were determined as follows. (i) The value of $\theta_{\mathrm{h}}$ was determined so that the imaginary part of the first term in the parentheses, which was measured experimentally, fit a linear function of $T$ at temperatures outside of the glass transition region. (ii) The values of $\eta_0$ and $\eta_1$ were determined to make the third term in the parentheses agree the linear function of $T$ found in the previous procedure. This made the imaginary part of $C^*_{\mathrm{liq}}$ be zero at temperatures outside of the glass transition region. (iii) The values of $\xi_0$ and $\xi_1$ were determined to make the second term in the parentheses fit the real part of the first term at temperatures lower than the glass transition temperature where the real part of $C^*_{\mathrm{liq}}$ should have been zero. (iv) The value of $|K_{\mathrm{h}}|$ was determined to scale the height of the stepwise change in the real part of $C^*_{\mathrm{liq}}$ to unity.

Before the aging the sample was heated to 120 °C at 1 K/min. Without duration the sample was cooled to the aging temperature at 0.5 K/min. Aging time dependence was studied with the fixed aging temperature of 90 °C. Aging time studied was 10, 30, 65 and 100 h. After the aging the sample was cooled to 60 °C at 0.5 K/min. Measurement on the heating process at 1 K/min started without duration. Results from this heating process were used in this work. Then the next cooling process with another aging condition started without duration. Measurement without aging was also made as the reference. The period of the temperature modulation was fixed to 10 s. The amplitude of the temperature modulation was 0.6 K at the room temperature and slightly smaller at higher temperatures. Reproducibility of the experimental results was confirmed by the last measurement with the same condition with the first one.

## 3. Results and discussion

Temperature dependence of the total thermal expansion coefficient ($\alpha_{\mathrm{tot}}$), the complex thermal expansion coefficient ($\alpha^*$) and the complex heat capacity ($C^*_{\mathrm{liq}}$) after aging at 90 °C for various periods are shown in Figs. 2–4, respectively. The aging period of each curve is explained in the figure caption. The total thermal expansion coefficient curves exhibit peaks attributed to the volume recovery of the aged sample. The peak becomes larger and the peak position shifts to the higher temperature with the aging time. These results are consistent with the conventional DSC results [17].

Both the complex thermal expansion coefficient and the complex heat capacity exhibited stepwise increase in the real part and a peak of the imaginary part as expected. The curves of Fig. 3(a) and (b) are similar in shape to those of Fig. 4(a) and (b), respectively. The complex thermal expansion coefficient and the complex heat capacity after aging for 100 h are compared to each other in Fig. 5. The complex thermal expansion coefficient shown in Fig. 5 was scaled after subtracting the contribution from the glass component as done for the complex heat capacity. It should be noted that the stepwise change in the real part of

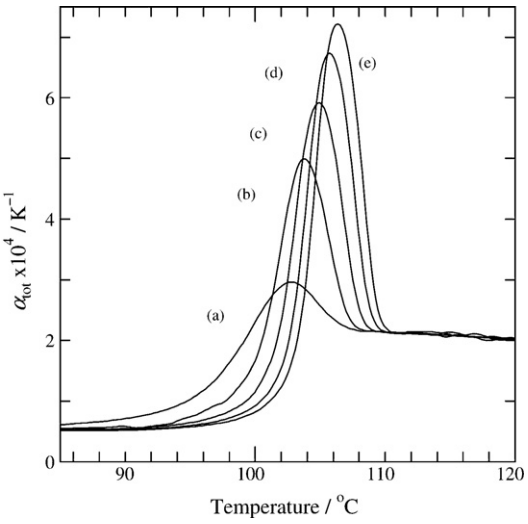


Fig. 2. Temperature dependence of the total thermal expansion coefficient on the heating process at 1 K/min after aging at 90 °C for (a) 0 h, (b) 10 h, (c) 30 h, (d) 65 h and (e) 100 h.

the complex thermal expansion coefficient occurred at a lower temperature than that of the complex heat capacity (Fig. 5(a)). The peak temperature of the imaginary part of the complex thermal expansion coefficient was lower than that of the complex heat capacity (Fig. 5(b)).

Temperature corresponding to the fictive temperature was estimated integrating the real part of the complex thermal expansion coefficient and the complex heat capacity. The calculated fictive temperature $T_{\mathrm{af}}$ is plotted against the aging period in Fig. 6. It should be noted that this temperature, called apparent fictive temperature, does not agree with the fictive temperature estimated from the total thermal expansion coefficient or the total heat flow. The apparent fictive temperature is higher than the fictive temperature because the complex thermal expansion coefficient and the complex heat capacity contain negligible contribution from the irreversible volume and enthalpy recoveries, respectively. Difference between $T_{\mathrm{af}}$ values, $\Delta T_{\mathrm{af}}$, of the complex thermal expansion coefficient and the complex heat capacity is also plotted in Fig. 6. It can be seen that the $T_{\mathrm{af}}$'s shifted to the higher temperature as the aging period became longer. $\Delta T_{\mathrm{af}}$ decreased until ca. 30 h but was almost constant at longer times.

The experimental results are discussed below from the view point of the energy landscape picture [18–21]. Since we measured temperature dependence of the thermal expansion coefficient and the heat capacity the following discussion is based on the free energy landscape [20,21] which depends on the temperature. In the glassy state the representative point of the system is trapped in a basin of the landscape. The free energy barriers surrounding the basin are too high to overcome. The glass transition observed in the heating condition is the process to release the degrees of freedom to jump from one basin to another. As the temperature increases the free energy barrier becomes lower. The area of the landscape over which the system can move in the measurement time scale, which is the modulation period in this case, extends quickly with the temperature.

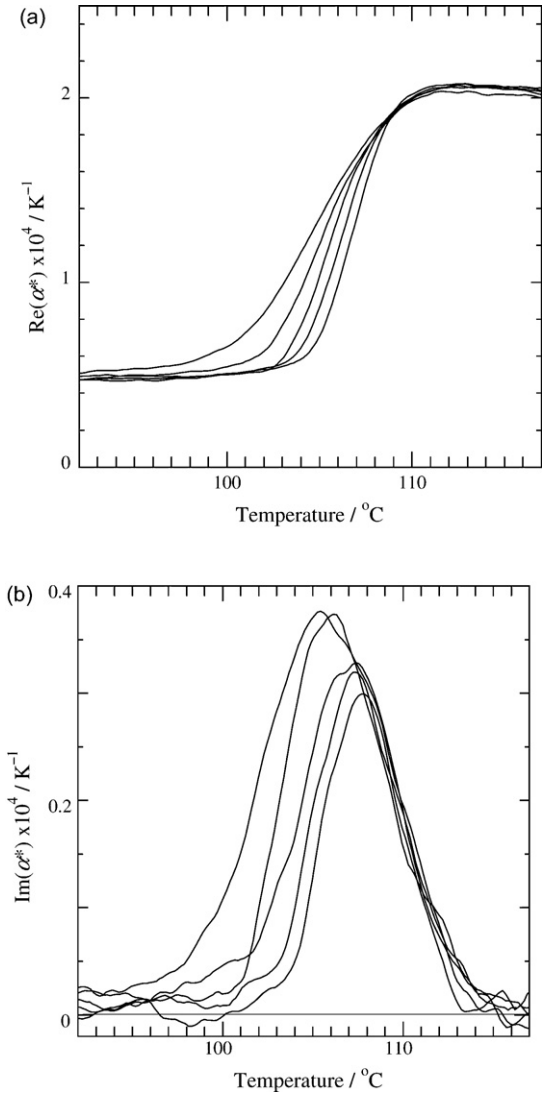


Fig. 3. Temperature dependence of the (a) real and (b) imaginary parts of the complex thermal expansion coefficient on the heating process at 1 K/min after aging at 90 °C for various periods. The aging periods of the five curves are 0, 10, 30, 65 and 100 h from the left to the right.

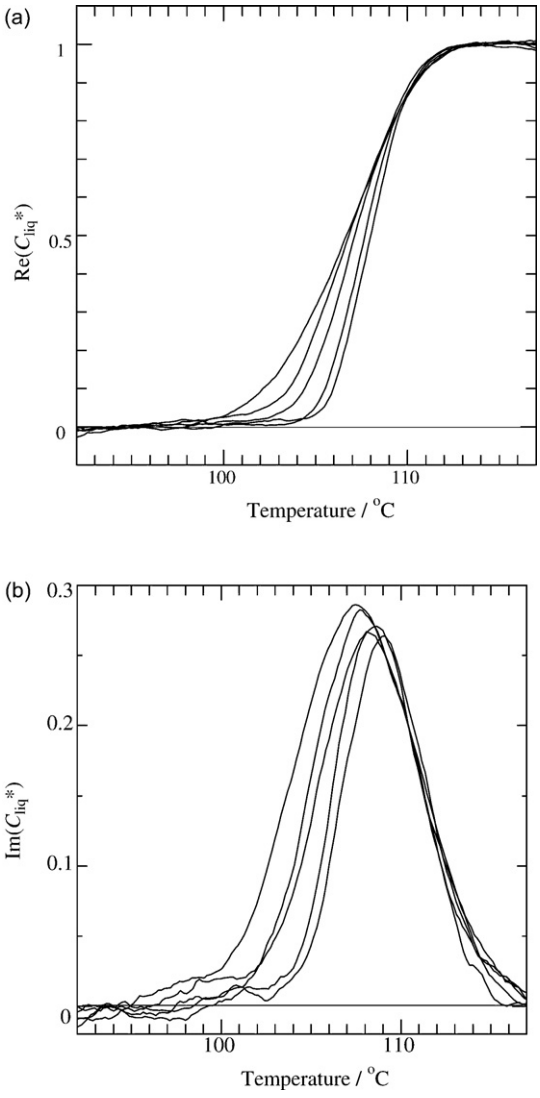


Fig. 4. Temperature dependence of the (a) real and (b) imaginary parts of the complex heat capacity on the heating process at 1 K/min after aging at 90 °C for various periods. The aging periods of the five curves are 0, 10, 30, 65 and 100 h from the left to the right.

Finally the system moves over the whole landscape freely and becomes liquid.

It is assumed that the free energy barrier between the neighboring basins with small difference of the free energy values is lower than that with large difference. Then at the initial stage of the glass transition the jumping motion between the basins with almost the same free energy values is activated. As temperature becomes higher the basins with higher free energy become accessible. Here we write the width of the free energy window where the accessible basins are distributed as $\Delta F$. $\Delta F$ is small at the initial stage of the glass transition. When $\Delta F$ is much smaller than $kT$, where $k$ and $T$ are Boltzmann's constant and temperature, respectively, the heat capacity due to the jumping motion is negligible. As the temperature becomes higher $\Delta F$ becomes larger and the heat capacity due to the jumping motion increases. At the final stage of the glass transition the free energy barrier is sufficiently low and $\Delta F$ is determined by the equilibrium Boltzmann distribution. Hereafter the heat capacity changes moderately with temperature.

The volume expansion coefficient is not directly connected to the energy landscape. However, it can be considered that the excess volume expansion accompanying the glass transition is induced by the jumping motion on the landscape. The simplest assumption is that the excess volume increases with the number of accessible basins. Then the excess volume expansion starts with the jumping motion even at a temperature where $\Delta F \ll kT$. This suggests that the change in the thermal expansion coefficient occurs at lower temperature than the change in the heat capacity. Therefore this model qualitatively explains the discrepancy between the thermal expansion coefficient and the heat capacity.

The aging effects can be explained consistently with the landscape picture as well. As shown in Figs. 3–6 the starting temperature of the change in the thermal expansion coefficient

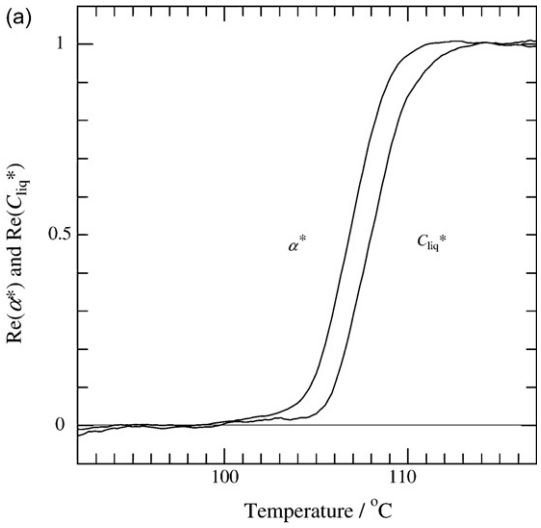


Fig. 5. Comparison of the complex thermal expansion coefficient ($\alpha$*) and the complex heat capacity ($C^*_{liq}$) after aging for 100 h. (a) The real part and (b) the imaginary part.

and the heat capacity shifted to higher temperature direction as the aging time increased at 90 °C. These effects can be attributed to growing of the free energy barriers with the aging time. It should be noted that the stepwise change in the real part of the complex thermal expansion coefficient and the heat capacity did not keep the curve shapes but sharpened. Sharpening of the stepwise change suggests that the lower energy barrier grows more than the higher energy barrier. Quantitative studies of this model will be reported elsewhere.

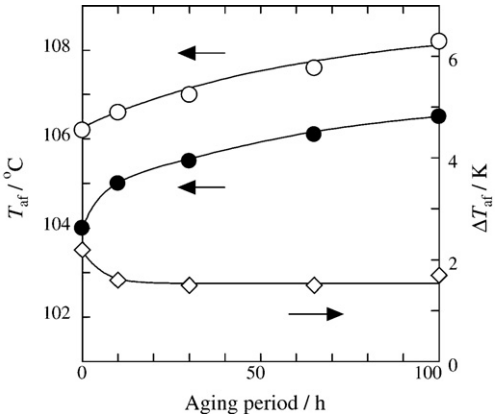


Fig. 6. $T_{af}$ of the complex thermal expansion coefficient (solid circles) and the complex heat capacity (open circles) plotted against the aging period. $\Delta T_{af}$ is shown with open diamonds.

## References

[1] Studies of the glass transition by many authors including the aging phenomena are reviewed for example in J. Mark, K. Ngai K., W. Graessley, L. Mandelkern, E. Samulski, J. Koenig, G. Wignall, Physical Properties of Polymers, 3rd ed., Cambridge, 2003, pp. 72–152.
[2] K. Takegawa, K. Fukao, Y. Saruyama, Thermochim. Acta 432 (2) (2005) 212.
[3] S. Takahara, M. Ishikawa, O. Yamamuro, T. Matsuo, J. Phys. Chem. B 103 (1999) 792.
[4] A. Toda, C. Tomita, M. Hikosaka, Y. Saruyama, Thermochim. Acta 324 (1–2) (1998) 95.
[5] A. Toda, T. Oda, M. Hikosaka, Y. Saruyama, Polymer Commun. 38 (1) (1997) 231.
[6] A. Hensel, J. Dobbertin, J.E.K. Schawe, A. Boller, C. Schick, J. Therm. Anal. 46 (1996) 935.
[7] J.M. Hutchinson, S. Montserrat, Thermochim. Acta 377 (2001) 63.
[8] C. Bauer, R. Böhmer, S. Moreno-Flores, R. Richert, H. Sillescu, D. Neher, Phys. Rev. E 61 (2000) 1755.
[9] K. Fukao, Y. Miyamoto, Phys. Rev. E 64 (2001) 011803.
[10] D.M. Price, J. Therm. Anal. Cal. 64 (2001) 323.
[11] D.M. Price, Thermochim. Acta 357–358 (2000) 23.
[12] D.M. Price, J. Therm. Anal. Cal. 51 (1998) 231.
[13] P. Kamasa, P. Myslinski, M. Pyda, Thermochim. Acta 442 (2006) 48.
[14] P. Kamasa, P. Myslinski, M. Pyda, Thermochim. Acta 433 (2005) 93.
[15] P. Myslinski, P. Kamasa, A. Wasik, M. Pyda, B. Wunderlich, Thermochim. Acta 392–393 (2002) 187.
[16] P. Myslinski, P. Kamasa, A. Wasik, Thermochim. Acta 387 (2002) 131.
[17] H. Yoshida, Netsusokutei 13 (1996) 193 (in Japanese).
[18] M. Goldstein, J. Chem. Phys. 51 (1969) 3728.
[19] F.H. Stillinger, T.A. Weber, Phys. Rev. A25 (1982) 978.
[20] M. Mézard, G. Parisi, J. Chem. Phys. 111 (1999) 1076.
[21] T. Tao, A. Yoshimori, T. Odagaki, Phys. Rev. E 66 (2002) 041103.